

Synthesis, Structure, and Oxidative Reactivity of a Class of Thiolate-Bridged Dichromium Complexes Featuring Antiferromagnetic Coupling Interactions

Nianmin Wei,^[a] Dawei Yang,^{*[a]} Yixin Zhang,^[a] Baomin Wang,^[a] and Jingping Qu^[a, b]

Several thiolate-bridged dichromium complexes with Cp* (Cp* = $\eta^5\text{-C}_5\text{Me}_5$) as auxiliary ligands were designed and synthesized through the salt metathesis, which all contain two six-coordinate chromium centers in the formal valence of +3. These complexes are all paramagnetic species, which are in good agreement with the experimental results that broad and paramagnetically shifted proton resonances appear in the ^1H NMR spectra. Furthermore, variable-temperature solid-state magnetic susceptibility studies reveal the two chromium centers of these complexes are both in an $S=3/2$ high-spin

state with a strong antiferromagnetic coupling. Simulated values of antiferromagnetic coupling constant for these complexes are directly related to the distances of the two Cr^{III} centers confirmed by X-ray crystallography. In addition, in the presence of dehalogenation agent AgPF₆, complexes [Cp*CrCl(μ -SR)₂CrClCp*] (3, R=Et; 4, R=ⁱPr) and [Cp*Cr(μ -Cl)(μ -SEt)₂CrCp*][BPh₄] (5) containing easily removable chloride can achieve the catalytic oxidation of organic substrates, such as PPh₃, 1,4-cyclohexadiene and 1,2-diphenylhydrazine under an oxygen atmosphere.

1. Introduction

Di- or multinuclear metal-sulfur clusters have constantly attracted considerable attention because of their vital roles in biological catalytic cycles.^[1] To date, a large variety of metal thiolate complexes have been designed and synthesized, which were commonly used as biomimetic structural and functional models of some important metalloenzymes^[2] or excellent catalysts for organic transformations.^[3] In sharp contrast to the great number and structural diversity of iron,^[4] molybdenum^[5] and nickel thiolate complexes,^[6] chromium thiolate complexes are only limited to a few systems,^[7] especially binuclear framework.^[8] However, chromium as a trace element in the life system plays important roles in maintaining proper carbohydrate and lipid metabolism.^[9] On the other hand, chromium complexes can also serve as excellent promoters for some catalytic transformations of organic substrates, especially oxidation.^[10] Therefore, construction of active thiolate-bridged binuclear chromium complexes is of significance to understand the functional nature of chromium metal.

Cyclopentadienyl and its derivatives have proven to be versatile ancillary ligands, because they possess unique electronic and steric tuning effects to control over reactivity and selectivity.^[11] Based on this understanding, the cyclopentadienyl

ligand was introduced as auxiliary ligands for construction of thiolate-bridged bimetallic complexes^[12] in the past decades which show the unique small molecule activation and transformation of organic substrates by the bimetallic cooperative effect.^[13] In contrast, only a few thiolate-bridged dichromium complexes with Cp* (Cp* = $\eta^5\text{-C}_5\text{Me}_5$) were reported by different research groups.^[14] However, to the best of our knowledge, all these thiolate-bridged dichromium complexes cannot accomplish catalytic transformation of organic substrates. This is attributed to the fact that the coordination spheres of these complexes are usually complemented by CO, sulfide or NO ligands, which commonly cannot be easily removed to provide the potential active site. In this context, it is very desirable to develop suitable thiolate-bridged dichromium systems possessing potential of catalytic transformation of small molecules.

In our previous work, a series of biomimetic thiolate-bridged diiron complexes or hetero-binuclear complexes containing iron using Cp* as auxiliary ligands were designed and constructed.^[15] In particular, thiolate-bridged diiron complexes as nitrogenase functional model showed excellent reactivity, which can realize the systematic simulation of the biological nitrogen fixation process and catalytic N–N bond cleavage of phenyl hydrazine to release aniline and ammonia.^[16] In order to pursue different catalytic properties, we adopted the strategy of tuning the metal center, and as expected, some unique catalytic properties were achieved in these new systems.^[17] As further extension of our work, mid-transition metal chromium was also considered. Herein, we report the preparation and characterization of several paramagnetic thiolate-bridged dichromium complexes with Cp* as auxiliary ligand, some of which feature the easily removable chloride groups. Interestingly, these complexes exhibit catalytic reactivity toward oxidation of organic substrates using O₂ as oxidant under mild conditions.

[a] N. Wei, Dr. D. Yang, Dr. Y. Zhang, Prof. B. Wang, Prof. J. Qu
State Key Laboratory of Fine Chemicals
Dalian University of Technology
Dalian, 116024, P. R. China
E-mail: yangdw@dlut.edu.cn
http://faculty.dlut.edu.cn/yangdawei/zh_CN/

[b] Prof. J. Qu
Key Laboratory for Advanced Materials
Shanghai, 200237, P. R. China

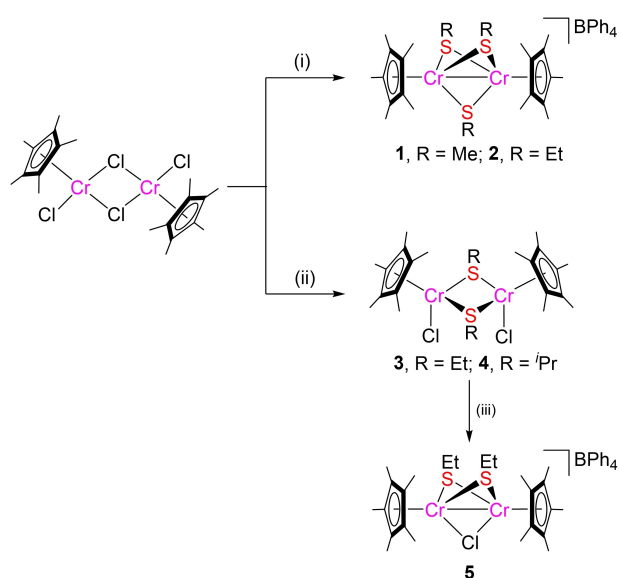
Supporting information for this article is available on the WWW under <https://doi.org/10.1002/ejic.202001050>

2. Results and Discussion

2.1. Synthesis and characterization of thiolate-bridged dichromium complexes

Initially, to introduce readily removable group for the potential active site, we chose chloride-bridged Cr^{III}Cr^{III} complex [Cp*CrCl(μ -Cl)₂ClCrCp*]^[18] as the precursor to construct thiolate-bridged dichromium complexes. As outlined in Scheme 1, treatment of [Cp*CrCl(μ -Cl)₂ClCrCp*] with 3 equiv. of NaSMe or LiSEt in the presence of stoichiometric NH₄PF₆, followed by counter anion exchange with 1 equiv. of NaBPh₄, facily generated thiolate-bridged dichromium complexes [Cp*Cr(μ -SR)₃CrCp*][BPh₄] (**1**, R = Me; **2**, R = Et) in good yields. Unexpectedly, when the substituent of the bridging thiolate ligand was changed to relatively more sterically hindered isopropyl, there is no analogue obtained under similar conditions. This experimental fact suggests the steric encumbrance plays a key role in the construction of the Cr₂S₃ core framework. Interestingly, when the dimer precursor [Cp*CrCl(μ -Cl)₂ClCrCp*] reacted with 2 equiv. of LiSEt or LiⁱPr from -78 °C to room temperature, novel thiolate-bridged dichromium complexes [Cp*CrCl(μ -SR)₂CrClCp*] (**3**, R = Et; **4**, R = ⁱPr) possessing easily removable chloride groups were smoothly produced. Moreover, complex **3** can further slowly react with 1 equiv. of NaBPh₄ at room temperature to afford dichromium chloride bridged complex [Cp*Cr(μ -Cl)(μ -SEt)₂CrCp*][BPh₄] (**5**). These complexes were found to be readily soluble in polar solvent such as THF and CH₂Cl₂, but with no dissolution in low polar solvent such as *n*-hexane. They are all robust whether in solution or in the solid-state under an inert atmosphere for a long time.

From simple charge balance consideration, the formal oxidation states of the two chromium centers in these five



Scheme 1. Synthesis of thiolate-bridged dichromium complexes **1-5**. Reagents and conditions: (i) 3 eq. NaSMe or LiSEt, 1 eq. NH₄PF₆, THF, -78 °C to rt, and 1 eq. NaBPh₄, CH₂Cl₂, 6 h (**1**, 71%; **2**, 76%); (ii) 2 eq. LiSEt or LiⁱPr, THF, -78 °C to rt (**3**, 47%; **4**, 75%); (iii) 1 eq. NaBPh₄, CH₂Cl₂, rt, 2 d, 91%.

complexes are all +3 valence. These complexes have been fully characterized by various spectroscopic methods. Similar to some other reported Cr^{III}Cr^{III} species,^[19] these complexes are all paramagnetic as evidenced by ¹H NMR spectroscopic data. The ¹H NMR spectrum of [Cr₂S₃]-type complex **1** shows two broad peaks at δ -0.87 and 2.20 ppm, which are likely to be attributed to methyl proton resonances of two equivalent Cp* and three bridging SMe ligands. As expected, there are also two broad peaks at δ -1.48 and 3.16 ppm with paramagnetic shift for methyl proton signals in the ¹H NMR spectrum of complex **2**. In addition, there is a very broad peak at around δ 3.31 ppm observed, which is probably assigned to the methylene protons of the three bridging SEt ligands based on the corresponding integration. Moreover, the ¹H NMR spectra of [Cr₂S₂]-type complexes **3** and **4** also exhibit two diagnostic broad peaks at δ -14.10, 14.31 and -19.81, 14.98 ppm. Differently, these two main resonances show a more obvious paramagnetic shift compared to complexes **1** and **2**, which are more difficult for further accurate assignment. Additionally, the ¹H NMR spectrum of **5** also shows two broad peaks at -4.45 and 3.83 ppm. Although above ¹H NMR data cannot provide suitable information for structural assignment, it is enough to distinguish these complexes. Moreover, the electrospray ionization high-resolution mass spectrometry (ESI-HRMS) data and elemental analysis provide further evidence for the molecular compositions of these complexes.

Furthermore, molecular structures of these complexes were unambiguously determined by single-crystal X-ray diffraction analysis. The ORTEP drawings of representative complexes **2**, **3** and **5** are shown in Figure 1, and selected bond distances and angles are listed in Table 1. These complexes are all coordinatively saturated with the two six-coordinate chromium centers in a tripod-like configuration. As shown in Figure 1a, the crystal structure of complex **2** owns a {Cr₂S₃} core framework, which resembles the other structurally similar dichromium^[20] and diiron^[12c] or diruthenium analogues.^[21] The two chromium centers are bridged through three thiolate ligands with the Cr-Cr vector serving as a pseudo-C₃ axis. The two Cp* ligands coordinate to the two chromium centers, respectively, and the two Cp* rings are almost parallel with the dihedral angle of only 2.9(2)°. The distance between the two chromium centers is 2.7601(8) Å, which is indicative of the presence of a metal-metal single bond.^[22] The average Cr-S bond is 2.361 Å, which

Table 1. Selected bond lengths (Å) and angles (°) of complexes **1-5**.

Complex	1	2	3	4	5
Cr1-Cr2	2.7489(7)	2.7601(8)	3.326(1)	3.3230(3)	2.7929(5)
Cr1-S1	2.368(2)	2.366(1)	2.4058(7)	2.4158(6)	2.3737(7)
Cr1-S2	2.378(1)	2.356(1)	2.3926(8)	2.4064(6)	2.3612(7)
Cr2-S1	2.384(1)	2.353(1)	2.3926(8)	2.4064(6)	2.3847(7)
Cr2-S2	2.398(1)	2.353(1)	2.4058(7)	2.4158(6)	2.3699(7)
Cr1-S3	2.317(1)	2.372(1)	-	-	-
Cr2-S3	2.321(1)	2.364(1)	-	-	-
Cr1-Cl1	-	-	2.2850(8)	2.2908(6)	2.3642(7)
Cr2-Cl2(Cl1)	-	-	2.2850(8)	2.2908(6)	2.3538(8)
Cr1-Cp*1	1.8753(6)	1.8906(5)	1.9120(7)	1.9287(1)	1.8675(6)
Cr2-Cp*2	1.8761(5)	1.8848(5)	1.9120(7)	1.9287(1)	1.8719(6)
Cp*1 [^] Cp*2	4.1(1)	2.9(2)	82.5(2)	83.3	3.8(1)

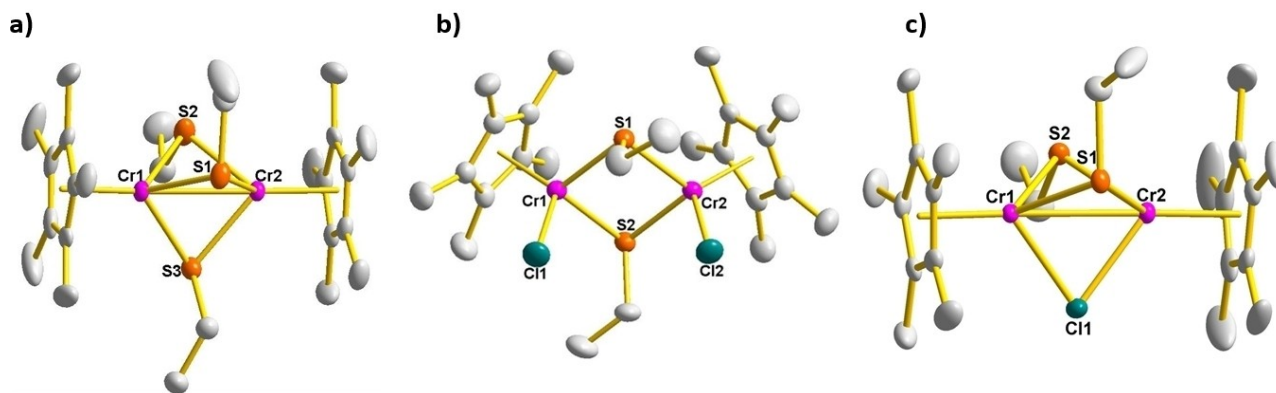


Figure 1. ORTEP (thermal ellipsoids at a 50% probability) diagrams of complexes **2** (a), **3** (b), and **5** (c). All hydrogen atoms and counter anions BPh_4^- are omitted for the sake of clarity.

falls in the common range of known thiolate-bridged dichromium complexes.^[20]

The solid-state structure of **3** clearly exhibits a butterfly-type $\{\text{Cr}_2\text{S}_2\}$ core skeleton, as shown in Figure 1b. Except for two mutually *cis* Cp* ligands and two SEt groups in different orientations, there also exist two terminal chlorides in the coordination spheres. Consequently, the distance between the chromium centers is significantly elongated to 3.326(1) Å compared with complexes **1** and **2**, which suggests there is no metal–metal bond interaction. Meanwhile, the dihedral angle between the two Cp* rings is increased to 82.5(2)°. The two Cr atoms and two sulfur atoms are nearly coplanar with the torsion angle of 179.40(7)°. In contrast with **3**, one terminal chloride group was removed from one chromium center, and the other chloride group is located between the two chromium centers of complex **5** (Figure 1c). As a consequence, the distance of the two chromium centers is significantly shortened with the Cr–Cr bond length of 2.7929(5) Å. Besides, the two Cp* ligands flip down with the dihedral angle between the Cp* rings of only 3.8(1)°.

2.2. Magnetic behavior

Complexes **1–5** all feature two six-coordinate formally Cr^{III} centers with a d^3 electronic configuration. To get deep insight into their electronic structures, variable-temperature dc magnetic susceptibility data of complexes **1–5** in the solid-state were collected from 3 to 300 K by SQUID (superconducting quantum interference device) magnetometry. The plots of molar magnetic susceptibility ($\chi_{\text{m}}T$) versus temperature for the representative Cr^{III}Cr^{III} complexes **3**, **4** and **5** are shown in Figure 2. As observed at 3 K, the $\chi_{\text{m}}T$ values of five complexes are all close to zero, which clearly indicates the ground states of these complexes are diamagnetic. As the temperature rose to 300 K, the $\chi_{\text{m}}T$ values gradually increased. For example, the $\chi_{\text{m}}T$ value of **2** increases from 0.02 $\text{cm}^3\text{mol}^{-1}\text{K}$ at 3 K to 0.71 $\text{cm}^3\text{mol}^{-1}\text{K}$ at 300 K. This value is significantly less than the spin-only value of 3.75 $\text{cm}^3\text{mol}^{-1}\text{K}$ expected for two

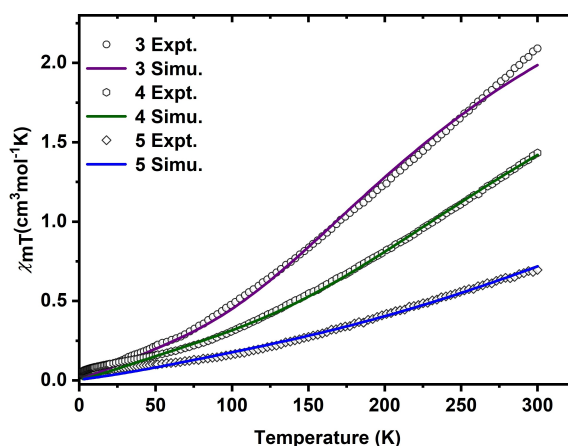


Figure 2. Variable-temperature dc magnetic susceptibility data for complexes **3–5**, and a theoretical fit of the experimental data.

magnetically isolated Cr^{III} centers in $S=3/2$ with $g=2.00$.^[23] Above experimental results suggests these dichromium systems populate the excited spin states of the spin ladder derived from the antiferromagnetic coupling of two Cr^{III} centers in $S=3/2$ as the temperature elevated. The similar phenomenon was also found in some other dichromium complexes with cyclopentadienyl ligands.^[8d,19a]

To quantify the strength of the antiferromagnetic coupling, their data were modeled with the program PHI^[24] to provide the corresponding exchange coupling constants (J_{12}). For instance, the J_{12} value of complex **1** is -107 cm^{-1} (Table 2) with $S_1=S_2=$

Table 2. The distances between the two chromium centers, exchange coupling constants and magnetic susceptibility for complexes **1–5**.

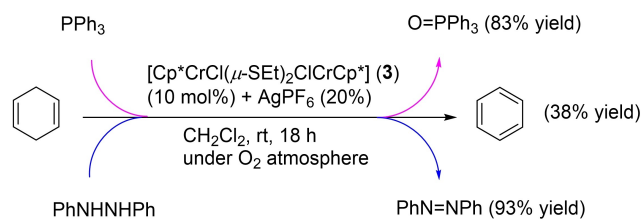
Complex	M···M distance [Å]	J_{12} [cm^{-1}]	$\chi_{\text{m}}T$ at 300 K [$\text{cm}^3\text{mol}^{-1}\text{K}$]
1	2.7489(7)	−107	0.65
2	2.7601(8)	−101	0.71
3	3.326(1)	−35	2.09
4	3.3230(3)	−54	1.43
5	2.7929(5)	−80	0.73

$3/2$, $g_1 = g_2 = 2.0$. Compared to complex **2** with $J_{12} = -101 \text{ cm}^{-1}$ and complex **5** with $J_{12} = -80 \text{ cm}^{-1}$, the relatively high value indicates the stronger antiferromagnetic coupling between the two Cr^{III} centers. Notably, the J_{12} values of -35 and -54 cm^{-1} for complexes **3** and **4** with longer metal–metal distances are remarkably smaller than those of complexes **1**, **2** and **5**, which indicates the elongation of the distance between the two Cr^{III} ions obviously weakens the antiferromagnetic coupling interaction.

These above results imply the J_{12} value is apparently associated with the distance between the two chromium centers as shown in Table 2. Similar direct correlation was also observed in other reported $\text{Cr}^{\text{III}}\text{Cr}^{\text{III}}$ complexes.^[19b,25] For example, the observed J_{12} value is up to -132 cm^{-1} in the hydroxide-bridged $\text{Cr}^{\text{III}}\text{Cr}^{\text{III}}$ complex $[\text{L}_2\text{Cr}^{\text{III}}_2(\mu\text{-OH})_3]_3 \cdot 3\text{H}_2\text{O}$ ($\text{L} = N, N', N''$ -trimethyl-1,4,7-triazacyclonane) with the short Cr–Cr bond length of $2.642(2) \text{ \AA}$.^[25a] However, the relatively longer distance between the two Cr^{III} centers of $3.197(3) \text{ \AA}$ in complex $[\text{Cr}_2(\text{dpa})_4][\text{OTf}]_2$ ($\text{dpa} = 2,2'$ -dipyridylamido) leads to a relatively small J_{12} value of -75 cm^{-1} .^[23]

2.3. Catalytic oxidative reactivity

To get one step further, the oxidative reactivity of these thiolate-bridged dichromium complexes was explored in the oxidation of triphenylphosphine (PPh_3) and the C–H or N–H bond activation of 1,4-cyclohexadiene (CHD) or 1,2-diphenylhydrazine (DPH) using dioxygen as oxidant. Initially, we carried out the control experiments in the absence of dichromium complexes as catalysts. The corresponding results of the spectroscopic analysis show there is no oxidized product obtained. Subsequently, the oxidative reactivity of these complexes toward above organic substrates using O_2 was examined under similar conditions. The $[\text{Cr}_2\text{S}_3]$ -type complexes **1** and **2** cannot realize the catalytic oxidation of above substrates. This experimental fact suggests the robustness of the three bridging thiolate ligands may hamper the coordination activation of substrates on the dichromium centers. Notably, complexes **3–5** bearing easily removable chloride ligands all can serve as catalysts for the oxidation of above substrates using O_2 in the presence of the halogen abstraction agent AgPF_6 . Among these thiolate-bridged dichromium complexes, complex **3** exhibits the best catalytic activity as shown in Scheme 2.



Scheme 2. Catalytic oxidative reactivity of complex **3** toward organic substrates under an oxygen atmosphere.

In the presence of 2 equiv. of AgPF_6 , complex **3** can promote the oxidation of PPh_3 under 1 atmosphere of O_2 at room temperature. The $^{31}\text{P}\{^1\text{H}\}$ NMR spectroscopic results show the formation of OPPh_3 as the oxidized product in 83% yield. Furthermore, the oxidative capacity of complex **3** was also applied to achieve the oxidative aromatization of 1,4-cyclohexadiene with weak C–H bond dissociation energies (BDE) of around 76 kcal/mol .^[26] Gas chromatography-mass spectrometry (GC-MS) analysis reveals that benzene can be only obtained in 38% yield from hydrogen atom abstraction reaction of CHD promoted by complex **3**. The low yield is attributed to the low conversion of CHD under this catalytic condition, which is evidenced by the experimental fact that most of the starting material remained unreacted. In addition, the catalytic reactivity of complex **3** toward oxidative dehydrogenation of DPH^[27] using O_2 was also investigated. Under similar conditions, corresponding product azobenzene was smoothly obtained in high yield, which is confirmed by ^1H NMR spectroscopy. Notably, complex **4** as a structural analogue of **3** shows poorer catalytic oxidative activity (**S1**), which indicates the substituent on the thiolate ligand has an obvious influence on the catalytic behaviors as found in other reported bimetallic catalytic system.^[28]

3. Conclusions

In summary, we have designed and synthesized several new thiolate-bridged dichromium complexes with Cp^* as auxiliary ligands, which were all well-defined by various spectroscopic and X-ray crystallographic methods. Magnetic studies clearly indicate these complexes all feature two six-coordinate formally Cr^{III} centers both in an $S = 3/2$ high-spin state with strong antiferromagnetic interaction. Notably, thiolate-bridged dichromium complexes **3**, **4** and **5** with easily removable chloride can serve as good promoters for the catalytic oxidation of PPh_3 and some organic compounds with weak C–H or N–H bonds using oxygen as oxidant. Interestingly, the substituent on the bridging thiolate ligands has an obvious influence on the catalytic efficiency. Further investigations on the detailed mechanism of this catalytic oxidation system and development of new functional complexes containing chromium for other catalytic transformations are underway.

Experimental Section

General Procedures: All manipulations were carried out under dry nitrogen or argon atmosphere by using standard Schlenk techniques. All solvents were dried and distilled over an appropriate drying agent under argon. CrCl_3 , NH_4PF_6 , AgPF_6 , MeSSMe , HSEt , HS^iPr , $^t\text{BuLi}$, PPh_3 , CHD and DPH were commercially available and used without further purification. Precursor $[\text{Cp}^*\text{CrCl}(\mu\text{-Cl})_2\text{ClCrCp}^*]$ was prepared according to the literature methods.^[18] The ^1H and $^{31}\text{P}\{^1\text{H}\}$ NMR spectra were recorded on a Bruker 400 Ultra Shield spectrometer. ESI-HRMS were recorded on a HPLC/Q-ToF micro spectrometer. Elemental analyses were performed on a Vario EL analyzer. Infrared spectra were recorded on a NEXVSTM FT-IR spectrometer. GC analyses were performed using an Agilent 6890 N

gas chromatography system equipped with an Agilent DB-5MS 30 m x 0.25 mm column and FID detector.

Magnetic measurement: Magnetic susceptibility data were collected using a Quantum Design MPMS XL-5 or PPMS-9T (EC-II) SQUID magnetometer. Measurements for all the samples were performed on microcrystalline powder restrained by a parafilm and loaded in a capsule. The magnetic susceptibility data were corrected for the diamagnetism of the samples using Pascal constants and the sample holder and parafilm by corrected measurement. The data were modelled with the program PHI to provide fit parameters.^[24]

X-ray crystallography

The data were obtained on a Bruker SMART APEX CCD diffractometer with graphite-monochromated Mo $K\alpha$ radiation ($\lambda = 0.71073 \text{ \AA}$). Empirical absorption corrections were performed using the SADABS program.^[29] Structures were solved by direct methods and refined by full-matrix least-squares based on all data using F^2 using SHELX97.^[30] All of the non-hydrogen atoms were refined anisotropically. All of the hydrogen atoms were generated and refined in ideal positions. Disordered atomic positions were split and refined using one occupancy parameter per disordered group.

Deposition Numbers 1947966 (for 1), 1947967 (for 2), 1947968 (for 3), 1947969 (for 4), and 1947970 (for 5) contain the supplementary crystallographic data for this paper. These data are provided free of charge by the joint Cambridge Crystallographic Data Centre and Fachinformationszentrum Karlsruhe Access Structures service www.ccdc.cam.ac.uk/structures.

Preparation of $[\text{Cp}^*\text{Cr}(\mu\text{-SMe})_3\text{CrCp}^*][\text{BPh}_4]$ (1). At -78°C , NH_4PF_6 (163 mg, 1 mmol) and NaSMe (210 mg, 3 mmol) were added to the THF (15 mL) solution of $[\text{Cp}^*\text{CrCl}_2]_2$ (516 mg, 1 mmol). The mixture was allowed to warm to room temperature and the color gradually changed from blue to purple. The resulting purple solution was evaporated to dryness. Then NaBPh_4 (342 mg, 1 mmol) and CH_2Cl_2 (15 mL) were added into the residue. After being stirred for 6 h, the solution was evaporated under reduced pressure. The residue was extracted with CH_2Cl_2 (20 mL) and then dried *in vacuo*. The resulting residue was further washed with Et_2O ($3 \times 5 \text{ mL}$), and then dried under vacuum. Addition of Et_2O to the concentrated THF solution afforded **1** (593 mg, 0.71 mmol, 71%) as dark black microcrystalline solids. $^1\text{H NMR}$ (400 MHz, CD_2Cl_2): δ -0.87 (br), 2.20 (br), 6.87 ($\text{BPh}_4\text{-CH}$), 7.02 ($\text{BPh}_4\text{-CH}$), 7.30 ($\text{BPh}_4\text{-CH}$). ESI-HRMS (m/z): Calcd. for $[\text{1-BPh}_4]^+$: 515.1025 ; Found: 515.1035 . IR (Film, cm^{-1}): 3054 , 2983 , 2915 , 1576 , 1479 , 1425 , 1378 , 995 , 733 , 705 , 612 . Anal. Calcd. for $\text{C}_{47}\text{H}_{59}\text{BCr}_2\text{S}_3$: C, 67.61 ; H, 7.12 . Found: C, 67.43 ; H, 7.43 .

Preparation of $[\text{Cp}^*\text{Cr}(\mu\text{-SEt})_3\text{CrCp}^*][\text{BPh}_4]$ (2) Using a procedure similar to that used for **1**, complex **2** was synthesized using LiSEt in 76% yield. $^1\text{H NMR}$ (400 MHz, CD_2Cl_2): δ -1.48 (br), 3.16 (br), 3.31 (br), 6.87 ($\text{BPh}_4\text{-CH}$), 7.03 ($\text{BPh}_4\text{-CH}$), 7.31 ($\text{BPh}_4\text{-CH}$). ESI-HRMS (m/z): Calcd. for $[\text{2-BPh}_4]^+$: 557.1495 ; Found: 557.1478 . IR (Film, cm^{-1}): 3051 , 2981 , 1575 , 1478 , 1426 , 1375 , 731 , 705 , 607 . Anal. Calcd. for $\text{C}_{50}\text{H}_{65}\text{BCr}_2\text{S}_3$: C, 68.47 ; H, 7.47 . Found: C, 68.26 ; H, 7.48 .

Preparation of $[\text{Cp}^*\text{CrCl}(\mu\text{-SEt})_2\text{CrClCp}^*]$ (3). At -78°C , LiSEt (136 mg, 2 mmol) was added to the THF (15 mL) solution of $[\text{Cp}^*\text{CrCl}_2]_2$ (516 mg, 1 mmol). The mixture was allowed to warm to room temperature. The resulting blue solution was evaporated to dryness under vacuum. Then the blue residue was extracted with CH_2Cl_2 (20 mL) followed by drying *in vacuo*. The resulting residue was further washed with Et_2O ($3 \times 5 \text{ mL}$), CH_3OH ($3 \times 5 \text{ mL}$) and dried *in vacuo*. Addition of *n*-hexane to the concentrated CH_2Cl_2 solution afforded **3** (267 mg, 0.47 mmol, 47%) as dark black microcrystalline solids. $^1\text{H NMR}$ (400 MHz, CDCl_3): δ -14.10 (br),

14.31 (br). IR (Film, cm^{-1}): 3113 , 2908 , 2849 , 1495 , 1448 , 1366 , 1248 , 1014 , 961 , 802 , 750 . Anal. Calcd. for $\text{C}_{24}\text{H}_{40}\text{Cl}_2\text{Cr}_2\text{S}_2$: C, 50.79 ; H, 7.10 . Found: C, 50.50 ; H, 7.15 .

Preparation of $[\text{Cp}^*\text{CrCl}(\mu\text{-S}^i\text{Pr})_2\text{CrClCp}^*]$ (4). Using a procedure similar to that used for **3**, complex **4** was synthesized using Li^iPr in 75% yield. $^1\text{H NMR}$ (400 MHz, CDCl_3): δ -19.81 (br), 14.98 (br). IR (Film, cm^{-1}): 2998 , 2899 , 2854 , 1488 , 1438 , 1366 , 1234 , 1145 , 1012 , 594 . Anal. Calcd. for $\text{C}_{26}\text{H}_{44}\text{Cr}_2\text{Cl}_2\text{S}_2$: C, 52.43 ; H, 7.45 . Found: C, 52.18 ; H, 7.44 .

Preparation of $[\text{Cp}^*\text{Cr}(\mu\text{-Cl})(\mu\text{-SEt})_2\text{CrCp}^*][\text{BPh}_4]$ (5). NaBPh_4 (58 mg, 0.17 mmol) was added to a solution of complex **3** (96 mg, 0.17 mmol) in CH_2Cl_2 (5 mL) at room temperature and stirred for 2 d. The solution color gradually changed from deep blue to purple. The resulting solution was filtered and the filtrate was collected followed by drying *in vacuo*. Then the residue was washed with *n*-hexane. Addition of *n*-hexane to the concentrated CH_2Cl_2 solution afforded **5** (131 mg, 0.15 mmol, 91%) as dark black microcrystalline solids. $^1\text{H NMR}$ (400 MHz, CD_2Cl_2): δ -4.45 (br), 3.83 (br), 6.87 ($\text{BPh}_4\text{-CH}$), 7.02 ($\text{BPh}_4\text{-CH}$), 7.31 ($\text{BPh}_4\text{-CH}$). ESI-HRMS (m/z): Calcd. for $[\text{5-BPh}_4]^+$: 531.1072 ; Found: 531.1084 . IR (Film, cm^{-1}): 3048 , 2978 , 2906 , 1582 , 1483 , 1422 , 1368 , 1247 , 1017 , 700 , 607 . Anal. Calcd. for $\text{C}_{48}\text{H}_{60}\text{BClCr}_2\text{S}_2$: C, 67.72 ; H, 7.10 . Found: C, 67.39 ; H, 7.36 .

General procedures for catalytic oxidation of substrates. PPh_3 (0.5 mmol), AgPF_6 (0.1 mmol for **3** and **4**, 0.05 mmol for **5**), complex **3**, **4** or **5** (0.05 mmol) and hexamethylbenzene (0.1 mmol) were added into 25 mL flame-dried Schlenk tube. The reaction mixture was frozen at -78°C and the headspace was evacuated under reduced pressure followed by the addition of O_2 (1 atm). Then 2 mL CH_2Cl_2 was added into the reaction mixture under O_2 atmosphere. The reaction mixture was allowed to warm to room temperature and be further stirred at room temperature for 18 h. The resulting solution was evaporated to dryness under vacuum. The residue was extracted with Et_2O and then dried *in vacuo*. The conversions of PPh_3 and yields of OPPh_3 were determined by ^1H spectroscopy using hexamethylbenzene as an internal standard.

CHD (0.5 mmol), AgPF_6 (0.1 mmol for **3** and **4**, 0.05 mmol for **5**), complex **3**, **4** or **5** (0.05 mmol) were added into 25 mL flame-dried Schlenk tube. The reaction mixture was frozen at -78°C and the headspace was evacuated under reduced pressure followed by the addition of O_2 (1 atm). Then 2 mL CH_2Cl_2 and 70 μL toluene were added into the reaction mixture under O_2 atmosphere. The reaction mixture was allowed to warm to room temperature and be further stirred at room temperature for 18 h. The mixture was filtered and the filtrate was collected for further GC analysis. The conversions of CHD and yields of benzene were determined by GC analysis using toluene as an internal standard.

DPH (0.5 mmol), AgPF_6 (0.1 mmol for **3** and **4**, 0.05 mmol for **5**), complex **3**, **4** or **5** (0.05 mmol) were added into 25 mL flame-dried Schlenk tube. The reaction mixture was frozen at -78°C and the headspace was evacuated under reduced pressure followed by the addition of O_2 (1 atm). Then 2 mL CH_2Cl_2 was added into the reaction mixture under O_2 atmosphere. The reaction mixture was allowed to warm to room temperature and be further stirred at room temperature for 18 h. The reaction solution was concentrated in vacuum. The residue was further purified by column chromatography using a mixture of ethyl acetate and petroleum ether (1:10) as eluent to give the desired product azobenzene in good isolated yields.

Acknowledgements

This work was supported by the National Natural Science Foundation of China (Nos. 21690064, 21571026, 21231003), the Program for Changjiang Scholars and Innovative Research Team in University (No. IRT13008), the "111" project of the Ministry of Education of China and the Fundamental Research Funds for the Central Universities (DUT19RC(3)013).

Conflict of Interest

The authors declare no conflict of interest.

Keywords: Chromium · S Ligands · Antiferromagnetic coupling interaction · Oxidation

- [1] a) J. C. Fontecilla-Camps, P. Amara, C. Cavazza, Y. Nicolet, A. Volbeda, *Nature* **2009**, *460*, 814–822; b) M. Can, F. A. Armstrong, S. W. Ragsdale, *Chem. Rev.* **2014**, *114*, 4149–4174; c) B. B. Wenke, T. Spatzal, *Metallocofactors that Activate Small Molecules* (Ed.: M. W. Ribbe), Springer Nature, Switzerland AG, **2019**, pp. 1–14.
- [2] a) S. C. Lee, W. Lo, R. H. Holm, *Chem. Rev.* **2014**, *114*, 3579–3600; b) U. Apfel, F. Y. Pétilion, P. Schollhammer, J. Talarmin, W. Weigand, *Bioinspired Catalysis Meta-Sulfur Complexes* (Ed.: W. Weigand, P. Schollhammer); WileyVCH, Weinheim, **2014**, pp. 79–103; c) D. Schilter, J. M. Camara, M. T. Huynh, S. Hammes-Schiffer, T. B. Rauchfuss, *Chem. Rev.* **2016**, *116*, 8693–8749; d) K. Tanifuji, Y. Ohki, *Chem. Rev.* **2020**, *120*, 5194–5251.
- [3] a) M. Hidai, S. Kuwata, Y. Mizobe, *Acc. Chem. Res.* **2000**, *33*, 46–52; b) L. Omann, C. D. F. Königs, H. F. T. Klare, M. Oestreich, *Acc. Chem. Res.* **2017**, *50*, 1258–1269.
- [4] a) Y. Li, T. B. Rauchfuss, *Chem. Rev.* **2016**, *116*, 7043–7077; b) I. Čorić, P. L. Holland, *J. Am. Chem. Soc.* **2016**, *138*, 7200–7211; c) S. Ohta, Y. Ohki, *Coord. Chem. Rev.* **2017**, *338*, 207–225.
- [5] F. Y. Pétilion, P. Schollhammer, J. Talarmin, *Coord. Chem. Rev.* **2017**, *331*, 73–92.
- [6] a) N. A. Eberhardt, H. Guan, *Chem. Rev.* **2016**, *116*, 8373–8426; b) S. Ogo, *Coord. Chem. Rev.* **2017**, *334*, 43–53.
- [7] a) D. Sellmann, M. Wille, F. Knoch, *Inorg. Chem.* **1993**, *32*, 2534–2543; b) T. D. Ju, K. B. Capps, R. F. Lang, G. C. Roper, C. D. Hoff, *Inorg. Chem.* **1997**, *36*, 614–621; c) Z. Weng, L. Y. Goh, *Acc. Chem. Res.* **2004**, *37*, 187–199.
- [8] a) T. J. Greenhough, B. W. S. Kolthammer, P. Legzdins, J. Trotter, *Inorg. Chem.* **1979**, *18*, 3543–3548; b) I. L. Eremenko, S. Rosenberger, S. E. Nefedov, H. Berke, V. M. Novotortsev, *Inorg. Chem.* **1995**, *34*, 830–840; c) D. Reardon, I. Kovacs, K. B. P. Ruppá, K. Feghali, S. Gambarotta, J. Petersen, *Chem. Eur. J.* **1997**, *3*, 1482–1488; d) A. A. Pasynskii, F. S. Denisov, Y. V. Torubaev, N. I. Semenova, V. M. Novotortsev, O. G. Ellert, S. E. Nefedov, K. A. Lyssenko, *J. Organomet. Chem.* **2000**, *612*, 9–13.
- [9] a) A. Levina, P. A. Lay, *Coord. Chem. Rev.* **2005**, *249*, 281–298; b) J. B. Vincent, *Dalton Trans.* **2010**, *39*, 3787–3794; c) J. B. Vincent, *The Bioinorganic Chemistry of Chromium*, Wiley, Chichester, UK, **2013**.
- [10] a) J. Muzart, *Chem. Rev.* **1992**, *92*, 113–140; b) K. M. Smith, *Coord. Chem. Rev.* **2006**, *250*, 1023–1031; c) M. Rosillo, G. Domínguez, J. Pérez-Castells, *Chem. Soc. Rev.* **2007**, *36*, 1589–1604; d) C. Bariashir, C. Huang, G. A. Solan, W. Sun, *Coord. Chem. Rev.* **2019**, *385*, 208–229.
- [11] a) W. J. Evans, B. L. Davis, *Chem. Rev.* **2002**, *102*, 2119–2136; b) M. Nishiura, F. Guo, Z. Hou, *Acc. Chem. Res.* **2015**, *48*, 2209–2220; c) T. Piou, T. Rovis, *Acc. Chem. Res.* **2018**, *51*, 170–180.
- [12] a) S. Dev, K. Imagawa, Y. Mizobe, G. Cheng, Y. Wakatsuki, H. Yamazaki, M. Hidai, *Organometallics* **1989**, *8*, 1232–1237; b) M. R. DuBois, B. Jagirdar, B. Noll, S. Dietz, *Syntheses, Structures and Reactions of Cyclopentadienyl Metal Complexes with Bridging Sulfur Ligands* (Ed.: E. I. Stiefel, K. Matsumoto); ACS SYMPOSIUM SERIES, Washington D.C., **1996**, pp. 269–281; c) Y. Chen, Y. Zhou, J. Qu, *Organometallics* **2008**, *27*, 666–671.
- [13] a) H. Matsuzaka, J. Qü, T. Ogino, M. Nishio, Y. Nishibayashi, Y. Ishii, S. Uemura, M. Hidai, *J. Chem. Soc. Dalton Trans.* **1996**, 4307–4312; b) Y. Inada, Y. Nishibayashi, M. Hidai, S. Uemura, *J. Am. Chem. Soc.* **2002**, *124*, 15172–15173; c) Y. Senda, K. Nakajima, Y. Nishibayashi, *Angew. Chem. Int. Ed.* **2015**, *54*, 4060–4064; *Angew. Chem.* **2015**, *127*, 4132–4136.
- [14] a) H. Brunner, J. Wachter, E. Guggolz, M. L. Ziegler, *J. Am. Chem. Soc.* **1982**, *104*, 1765–1766; b) W. A. Herrmann, J. Rohrmann, H. Nöth, C. K. Nanila, I. Bernal, M. Draux, *J. Organomet. Chem.* **1985**, *284*, 189–211; c) G. Jin, M. Herberhold, *Trans. Metal Chem.* **2001**, *26*, 445–447; d) K. Sukcharoenphon, T. D. Ju, K. A. Abboud, C. D. Hoff, *Inorg. Chem.* **2002**, *41*, 6769–6774.
- [15] a) Y. Chen, Y. Zhou, P. Chen, Y. Tao, Y. Li, J. Qu, *J. Am. Chem. Soc.* **2008**, *130*, 15250–15251; b) D. Yang, Y. Li, B. Wang, X. Zhao, L. Su, S. Chen, P. Tong, Y. Luo, J. Qu, *Inorg. Chem.* **2015**, *54*, 10243–10249; c) P. Sun, D. Yang, Y. Li, Y. Zhang, L. Su, B. Wang, J. Qu, *Organometallics* **2016**, *35*, 751–757; d) Y. Zhang, D. Yang, Y. Li, X. Zhao, B. Wang, J. Qu, *Catal. Sci. Technol.* **2019**, *9*, 6492–6502.
- [16] a) Y. Chen, L. Liu, Y. Peng, P. Chen, Y. Luo, J. Qu, *J. Am. Chem. Soc.* **2011**, *133*, 1147–1149; b) Y. Li, Y. Li, B. Wang, Y. Luo, D. Yang, P. Tong, J. Zhao, L. Luo, Y. Zhou, S. Chen, F. Cheng, J. Qu, *Nat. Chem.* **2013**, *5*, 320–326.
- [17] a) Y. Zhang, P. Tong, D. Yang, J. Li, B. Wang, J. Qu, *Chem. Commun.* **2017**, *53*, 9854–9857; b) X. Zhao, D. Yang, Y. Zhang, B. Wang, J. Qu, *Org. Lett.* **2018**, *20*, 5357–5361; c) J. Li, D. Yang, P. Tong, C. Wang, B. Wang, J. Qu, *Inorg. Chem.* **2020**, *59*, 8203–8212.
- [18] D. S. Richeson, J. F. Mitchell, K. H. Theopold, *Organometallics* **1989**, *8*, 2570–2577.
- [19] a) A. A. Pasynskii, I. L. Eremenko, Y. V. Rakin, V. M. Novotortsev, V. T. Kalinnikov, G. G. Aleksandrov, Y. T. Struchkov, *J. Organomet. Chem.* **1979**, *165*, 57–64; b) K. H. Theopold, *Acc. Chem. Res.* **1990**, *23*, 263–270; c) M. A. Hutton, J. C. Durham, R. W. Grady, B. E. Harris, C. S. Jarrell, J. M. Mooney, M. P. Castellani, A. L. Rheingold, U. Kölle, B. J. Korte, R. D. Sommer, G. T. Yee, J. M. Boggess, R. S. Czernuszewicz, *Organometallics* **2001**, *20*, 734–740; d) P. Wei, D. W. Stephan, *Organometallics* **2003**, *22*, 1712–1717.
- [20] a) L. Y. Goh, M. S. Tay, T. C. W. Mak, R. Wang, *Organometallics* **1992**, *11*, 1711–1717; b) M. L. Ooi, C. E. Lim, R. C. S. Wong, S. W. Ng, *Inorg. Chim. Acta* **2017**, *467*, 364–371.
- [21] S. Dev, Y. Mizobe, M. Hidai, *Inorg. Chem.* **1990**, *29*, 4797–4801.
- [22] R. H. D. Lyngdoh, H. F. Schaefer, III, R. B. King, *Chem. Rev.* **2018**, *118*, 11626–11706.
- [23] D. W. Brogden, Y. Turov, M. Nippe, G. L. Manni, E. A. Hillard, R. Clérac, L. Gagliardi, J. F. Berry, *Inorg. Chem.* **2014**, *53*, 4777–4790.
- [24] a) N. F. Chilton, R. P. Anderson, L. D. Turner, A. Soncini, K. S. Murray, *J. Comput. Chem.* **2013**, *34*, 1164–1175; b) A. K. Hickey, S. M. Greer, J. A. Valdez-Moreira, S. A. Lutz, M. Pink, J. A. DeGayner, T. D. Harris, S. Hill, J. Telsler, J. M. Smith, *J. Am. Chem. Soc.* **2019**, *141*, 11970–11975.
- [25] a) A. Niemann, U. Bossek, K. Wiegardt, C. Butzlaff, A. X. Trautwein, B. Nuber, *Angew. Chem. Int. Ed.* **1992**, *31*, 311–313; *Angew. Chem.* **1992**, *104*, 345–348; b) R. Clérac, F. A. Cotton, C. A. Murillo, X. Wang, *Chem. Commun.* **2001**, 205–206; c) A. Døssing, *Coord. Chem. Rev.* **2014**, *280*, 38–53.
- [26] X. Xue, P. Ji, B. Zhou, J. Cheng, *Chem. Rev.* **2017**, *117*, 8622–8648.
- [27] T. Fujii, S. Yamaguchi, S. Hirota, H. Masuda, *Dalton Trans.* **2008**, 164–170.
- [28] a) J. Qü, D. Masui, Y. Ishii, M. Hidai, *Chem. Lett.* **1998**, *27*, 1003–1004; b) P. Sun, D. Yang, Y. Li, B. Wang, J. Qu, *Dalton Trans.* **2020**, *49*, 2151–2158.
- [29] G. M. Sheldrick, *SADABS, Program for area detector adsorption correction*, Institute for Inorganic Chemistry, University of Göttingen: Germany, **1996**.
- [30] a) G. M. Sheldrick, *SHELXL-97, Program for refinement of crystal structures*, University of Göttingen, Germany, **1997**; b) G. M. Sheldrick, *SHELXS-97, Program for Solution of Crystal Structures*, University of Göttingen, Germany, **1997**.

Manuscript received: November 17, 2020
Revised manuscript received: December 9, 2020
Accepted manuscript online: December 11, 2020